İSTANBUL UNIVERSITY
CERRAHPAŞA

RESEARCH ARTICLE

Electrica 2021; 21(1): 1-9

Performance Analysis of Implanted Hybrid Three Quasi Z source Inverter designed for Renewable Energy Conversion Applications

Ramanjaneyulu Alla, Anandita Chowdhury

Department of Electrical Engineering, Sardar Vallabhbhai National Institute of Technology, Surat, India

Cite this article as: Alla R, Chowdhury A. Performance Analysis of Implanted Hybrid Three Quasi Z source Inverter designed for Renewable Energy Conversion Applications. *Electrica*, 2021; 21(1): 1-9.

ABSTRACT

Implanted hybrid three quasi Z source inverter has been designed to achieve high voltage gain for a single-stage power conversion system. The net input voltage applied to the converter is the sum of the voltages of four independent sources to which the converter is configured. It is a fact that the power from renewable energy sources will not be constant and varies. So there is uncertainty in the uniform availability of energy from renewable energy sources and the resulting voltage variations in any of the four sources affects net input voltage of the converter. A dual-loop control method has been developed to control the dc-link voltage across the converter to attain a constant ac output voltage across load terminals and meet load requirements. The controller maintains the stable operation of the converter in the absence of any of the four voltage sources. Simulation results using MATLAB software are presented for the validation of the proposed work under the conditions of input voltage variations as well as a sudden change of loads.
Keywords: Shoot-through duty ratio, modulation index, simple boost control, voltage gain, Z source converter

Corresponding Author:
Ramanjaneyulu Alla

E-mail:
ramanjaneyulualla@gmail.com

Received: 03.09.2019

Accepted: 12.07.2020

Available Online Date: 10.09.2020

DOI: 10.5152/electrica.2020.19068

Introduction

Power converters are utilized to extract the maximum power from renewable energy sources (RES). In general, the voltage magnitude at the renewable energy extraction system is at a lower value. So power converters with high voltage gain are required to extract energy from renewable sources. Conventional voltage source and current source converters need secondary power conversion circuits to either reduce or boost the input voltage. These conventional converters have operational limitations and can be overcome by the impedance source converters (ISC). The first ISC is known as Z source converter (ZSC) [1]. The problems encountered in ZSC are solved in a quasi-Z source converter (QZSC) [2] and it has ZSC features. Now many configurations of ISC are developed to enhance the converter voltage gain and are reviewed in [3].

Magnetically coupled ISC (MCISC) are discussed in [4] which provide high voltage gains by changing the turns ratio value of the coupled coils and shoot-through duty ratio (*D*) value. In MCISC, higher voltage gains are achieved at higher modulation index (*m*) by varying turns ratio of the coils rather than *D*, Converters [4] are designed with a lesser number of circuit elements to get increase in voltage gain. Apart from these advantages, MCISC experiences startling voltage spikes [5] at dc-link terminals due to magnetic leakage. MCISC need clamping circuits [6] to reduce the voltage spikes. The addition of the clamping circuits increases the number of components in converter configuration. The review of pulse width modulation (PWM) methods [7] designed for ISC is discussed. Most researchers use the simple boost control method (SBC) method, as its implementation is very easy. The applications of ZSC in motor drive applications are illustrated in [8]. The application of ZSC for reactive power compensation [9] was explained.

Steady ac voltage across the connected load or for grid-connected applications is needed to regulate the dc-link voltage of the converter. As the dc-link voltage varies from zero to a peak value, the capacitor voltage is considered as a feedback voltage, both of them are expressed in terms of *D*. Controlling the dc-link voltage with improved transient response [10] was discussed, but the effect of inductor current ripples are not considered. The inductor current

ripples are controlled in the inner loop and dc-link voltage is controlled in the outer loop [11] with the implementation of dual-loop digital control.

Hybrid three quasi Z source dc-dc converter provides higher voltage gain [12]. Z source half-bridge inverter [13] has been designed to reduce voltage stress on capacitors and the cascade connection with the inverter was presented to get the higher voltage gain. An embedded ZSC [14] is formed by placing the half dc voltage at the inductors helps to draw smoother current at a voltage gain equals to the voltage gain in ZSC. Further, various topologies are designed to address the various network problems [15-20], resulting in improving the voltage gain of the ISC. Still, research is continuing toward the development of high gain and efficient topologies. The ISC working at low power factor loads or lower inductance value in the impedance network of the converter causes higher current ripples, as the converter might be working in discontinuous conduction mode [21].

Implanted hybrid three quasi Z source Inverter (ImHTQZSI) [15] is developed by using hybrid three quasi Z source dc-dc converter [12] by connecting four individual voltage sources in series with the inductors in impedance circuit. Although MCISC provides higher gain, it faces the voltage spikes at dc-link terminals. So clamping circuits are required to reduce voltage spikes in MCISC and it makes the circuit very complex. Hence, ImHTQZSI has been considered as it provides higher voltage gain compared with existing non-coupled coil ISC. This paper illustrates the configuration of ImHTQZSI and operating modes in Section 2. Input voltage disturbances due to uncertainties in the renewable energy sources are controlled by using a dual-loop control method on the dc-side of the converter is explained in Section 3. The performance of the converter with simulation results in the proposed control method is discussed in Section 4.

Configuration and Working of Proposed Inverter

QZSC with two configurations of the [2] are used to develop the present converter is shown in Figure 1. Here V_1, V_2, V_3, and V_4 are the dc voltage sources extracted from either renewable energy sources or direct dc sources. The network having components L_1, C_1, D_1, L_2, and C_2 represent the discontinuous current mode (DCM) operation of [2]. Similarly, the network formed with L_3, C_5, D_3, L_4, and C_6 is another DCM [2]. The final appearance of the converter with C_3, C_4, and diode D_2 is visualized as continuous current QZSC [2]. As a whole, the present QZSC has three configurations. A dc voltage source in series with the inductor is connected to get continuous input current from the sources. It can work in two modes; in one mode it works as normal inverter at both active and zero states known as the non-shoot-through state and in the second mode an extra zero state is added known as shoot-through zero state.

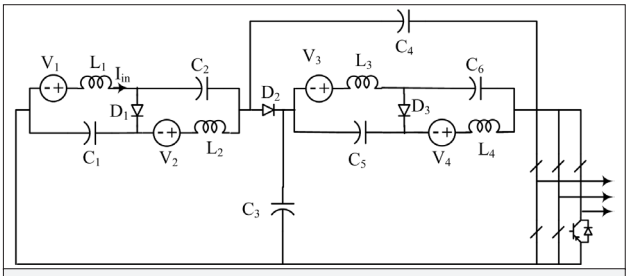

Figure 1. Implanted Hybrid Three Quasi Z source Inverter

Mode-1— Shoot-through zero state

The equivalent circuit of Figure 1 in shoot-through zero state operation is shown in Figure 2. In this mode all diodes are in off state and the converter terminals are short-circuited during the interval of T_{st} in a switching period of T. Converter terminals are short-circuited with turning on all switching devices at any of the leg or all legs or combination of legs. In mode-1, the inductors are energized by the capacitors leading to increase in current passing through inductors.

The voltage across the inductors in mode-1 is expressed in equations (1)–(4). Here V_{L1}, V_{L2}, V_{L3}, and V_{L4} are voltage across the respective inductors. Similarly V_{C1}, V_{C2}, V_{C3}, V_{C4}, V_{C5}, and V_{C6} are voltage across the respective capacitors.

$$V_{L1}=V_1+V_{C2}+V_{C4} \quad (1)$$

$$V_{L2}=V_2+V_{C1}+V_{C4} \quad (2)$$

$$V_{L3}=V_3+V_{C3}+V_{C6} \quad (3)$$

$$V_{L4}=V_4+V_{C3}+V_{C5} \quad (4)$$

Mode-2— non-shoot-through state

In non-shoot-through state all the diodes are on state and converter terminals are connected to load. They are represented with an equivalent current source shown in Figure 3 at a terminal voltage of V_{LK} during the interval of T_{nst} in a switching period of T. In this mode switching will happen as in conventional voltage source converter. The voltage across the inductors in mode-2 is expressed in equations (5)–(8). V_{LK} is the voltage across the dc-link terminals of the converter.

$$V_{L1}=V_1-V_{C1} \quad (5)$$

$$V_{L2}=V_2-V_{C2} \quad (6)$$

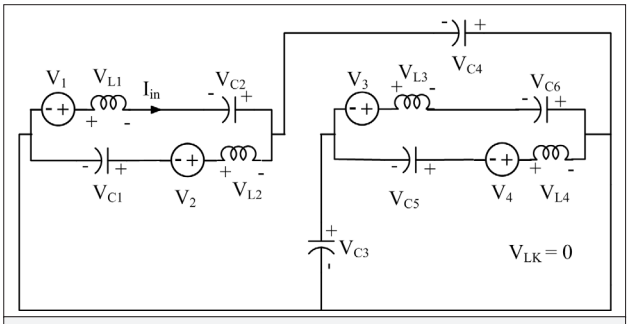

Figure 2. Mode-1 representation of ImHTQZSI

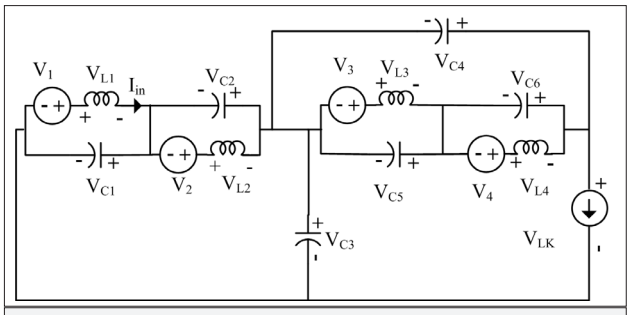

Figure 3. Mode-2 representation of ImHTQZSI

$$V_{L3}=V_3-V_{C5} \quad (7)$$

$$V_{L4}=V_4-V_{C6} \quad (8)$$

$$V_{C3}+V_{C4}=V_{LK} \quad (9)$$

The shoot-through duty ratio of the converter is represented as

$$D=\frac{T_{st}}{T} \quad (10)$$

According to volt-second balance principle across the inductor, the individual capacitor and dc-link voltages are expressed in equations (11) – (17)

$$V_{C1}=\frac{1-D}{1-2D}V_1+\frac{D}{1-2D}V_2+\frac{D}{1-2D}V_{C4} \quad (11)$$

$$V_{C2}=\frac{D}{1-2D}V_1+\frac{1-D}{1-2D}V_2+\frac{D}{1-2D}V_{C4} \quad (12)$$

$$V_{C3}=\frac{1-2D}{1-4D}(V_1+V_2)+\frac{2D}{1-4D}(V_3+V_4) \quad (13)$$

$$V_{C4}=\frac{2D}{1-4D}(V_1+V_2)+\frac{1-2D}{1-4D}(V_3+V_4) \quad (14)$$

$$V_{C5}=\frac{1-D}{1-2D}V_3+\frac{D}{1-2D}V_4+\frac{D}{1-2D}V_{C3} \quad (15)$$

$$V_{C6}=\frac{D}{1-2D}V_3+\frac{1-D}{1-2D}V_4+\frac{D}{1-2D}V_{C3} \quad (16)$$

$$V_{LK}=\frac{\sum_{i=1}^{4}V_i}{(1-4D)} \quad (17)$$

Equation (17) indicates the relation between dc-link voltage of the converter and four dc voltage sources. The net input dc voltage applied to the converter is the sum of the voltages of four individual dc sources as seen in equation (18).

$$V_{LK}=BV_{dc}$$

$$V_{dc}=\sum_{i=1}^{4}V_i \quad (18)$$

$$B=\frac{1}{(1-4D)} \quad (19)$$

where *B* denotes the voltage boost factor.

The value of inductances L_1-L_4 are considered according to equation (20)

$$L_i=\frac{v_{L,i}DT}{\%i_{L,i}} \quad \text{i=1,2,3, and 4} \quad (20)$$

Where $\%i_{L,i}$ is the percentage of ripple allowed in the corresponding inductor current.

The value of capacitances C_1-C_6 is considered according to equation (21)

$$C_i=\frac{i_{C,i}DT}{\%v_{C,i}} \quad \text{i=1,2,3, 4, 5, and 6} \quad (21)$$

Where $i_{C,i}$ is current through the ith capacitor and $\%v_{C,i}$ is the percentage of ripple allowed in the corresponding capacitor voltage.

Dual-Loop Control of ImHTQZSI

The family of ISC is designed to provide a high voltage gain in a single-stage conversion system. In this circuit, shoot-through zero state is inserted in place of conventional zero states to get boost voltages at dc-link. Three basic PWM methods, namely, SBC [2, 7], maximum boost control, and maximum constant boost control methods are used to get a peak output ac voltage from a boosted dc-link voltage. This paper uses SBC method to show the ImHTQZSI performance.

The relation between *m* and *D* in SBC control is

$$D+m=1 \quad (22)$$

Output peak ac voltage can be represented as

$$V_{ac}=m\frac{V_{LK}}{2} \quad (23)$$

The disturbances on input energy sources cause fluctuations in dc voltage across the converter terminals, which in turn vary the output ac voltage. To get a steady output ac voltage, the designer needs to control dc-link voltage by controlling '*D*' on dc-side and load disturbances on ac-side by controlling '*m*'.

Dc-side control

Dc-link voltage V_{LK} is maintained on dc-side to make the converter to provide required v_{ac}, according to equation (23). V_{LK} depends on *D*. V_{LK} is varying from zero to a peak value just like a pulse signal. V_{LK} is zero in STS and has a finite value in nSTS state. One PI controller is enough to control V_{LK}, by sensing the peak value of the dc-link voltage. For that, an extra sensing circuit is required. To avoid more or additional sensing circuit, capacitor voltage V_{C3} is considered to control V_{LK}, as V_{LK} and capacitor voltages are functions of *D*. One more PI controller is considered to control inductor current ripples and the bandwidth of the overall controller is increased [10, 11]. Hence two PI controllers required. V_{C3} *is* considered as a feedback element instead of V_{LK}, *and* it means indirect controlling of dc-link voltage as shown in Figure 4. Apart

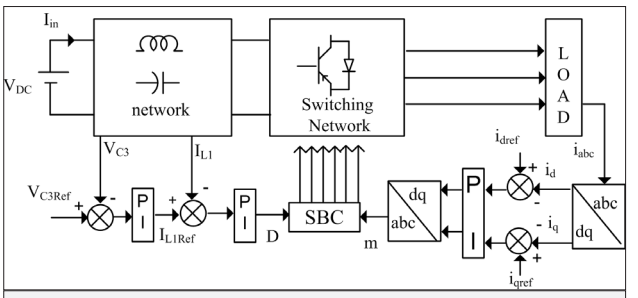

Figure 4. Dual Loop Control of of ImHTQZSI

from controlling V_{LK}, inductor current ripples are also regulated with the inner current loop. The outcome of the dc-side control is *D*. Outer voltage loop provides reference inductor current (I_{Lref}) given in equation (24) where *S* is the load in volt-amperes.

$$I_{Lref}=\frac{S}{\sum_{i=1}^{4}V_i} \quad (24)$$

Ac-side control

Load currents i_{abc} are considered as a feedback signal to generate modulating signals. The load current and its reference currents are transformed into *dq* components and are supplied to PI control. The output of PI control is then converted into *abc* components to provide modulating signals as shown in Figure 4. With the interaction of *m* and *D* values in the SBC method, the converter operates at a steady operating point. *D* and *m* are interrelated, as seen from equation (22). Disturbances on the dc-side of the converter influence ac-side performance of the converter as well as disturbances on the ac-side are also affect dc-side performance.

The reference peak ac current (i_{peak}) given in equation (25)

$$i_{peak}=\sqrt{2}\frac{P}{\sqrt{3}V_l cos\varphi} \quad (25)$$

Here V_l is the line voltage and $cos\varphi$ is the load power factor.

Table 1. System parameters

Parameter	Value
Inductance	2 mH
Capacitance	470 µf
Internal Resistance of Inductor	0.1 Ω
Internal Resistance of Capacitor	0.1 Ω
Switching Frequency	10 kHz
Output Voltage	70.7 V(ph)
Load	250-375 VA, 0.8 pf lag

The voltage stress across the switching devices are expressed in equation (26)

$$V_{D1}=V_{D2}=V_{D3}=V_{SW}=V_{LK}=\frac{\sum_{i=1}^{4}V_i}{1-4D} \quad (26)$$

Here V_{SW} is the voltage stress across the switches in the inverter

The current stress across the switching devices are expressed in equation (27)

$$i_{D1}=i_{D2}=i_{D3}=\frac{I_{in}}{1-D} \quad (27)$$

Simulation Results

The performance of the proposed converter with the dual-loop control method has to be tested and is carried out with MATLAB/simulink. The system parameters are listed in Table 1. Here step change in applied input voltage and load volt-ampere are considered disturbances for the validation of the controller

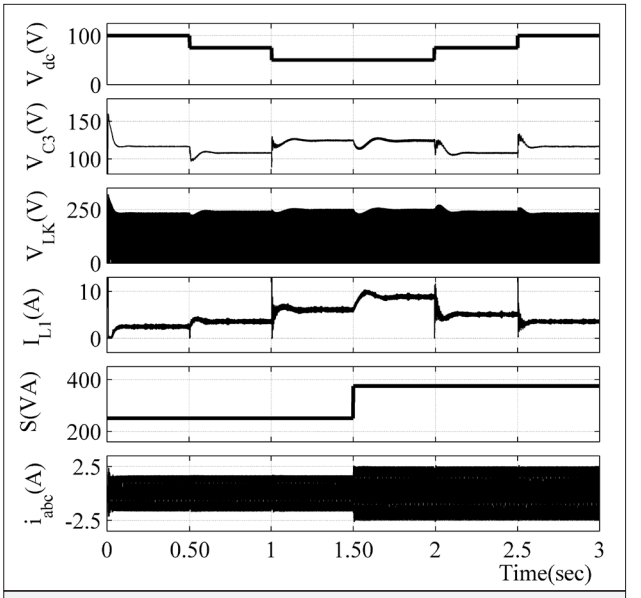

Figure 5. Steady state response of ImHTQZSI to step change in dc voltage and load VA

Table 2. Variation of converter parameters with input voltage and load changes

V_1	V_2	V_3	V_4	VC_3	VC_4	V_{LK}	*D*	*G*	*S*	i_{abc}
25	25	25	25	116.7	116.7	233.3	0.143	2	250	1.67
25	0	25	25	108.5	133.5	241.9	0.173	2.67	250	1.67
25	0	0	25	125	125	250	0.2	4	250	1.67
25	0	0	25	125	125	250	0.2	4	375	2.5
25	0	25	25	108.5	133.5	241.6	0.173	2.67	375	2.5
25	25	25	25	116.7	116.7	233.3	0.143	2	375	2.5

V_1, V_2, V_3 and V_4 are the input side dc source voltages in volts. V_{C3} and V_{C4} are the voltage across the capacitors C_3 and C_4 in volts. V_{LK} is the voltage across the dc- link terminals in volts. *D*, *G* and *S* are the shoot-through duty ratio, Converter voltage gain and load Volt-Amperes, respectively. i_{abc} is the current through the load in amperes.

performance. Figure 5 shows the steady-state response of the converter with disturbances at every 0.5 sec and the performance details are given in Table 2.

There is no load change in ac-side of the converter for 0 to 1.5 sec when input dc voltages are reduced by 25V at every 0.5 sec. At 1.5 sec load is increased by 50% and after at every 0.5sec dc voltage is increased by 25V. In all the cases, the converter meets the load requirements with four dc sources or three dc sources or two dc sources.

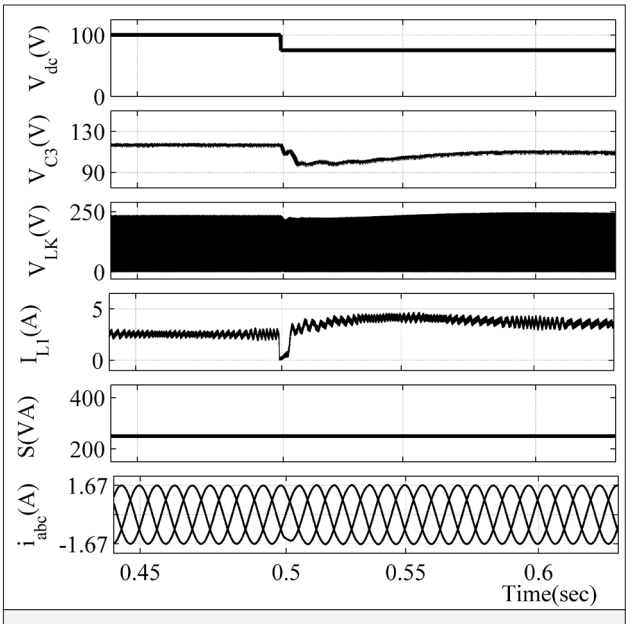

Figure 6. Response of ImHTQZSI at 100V to 75V step change in dc voltage

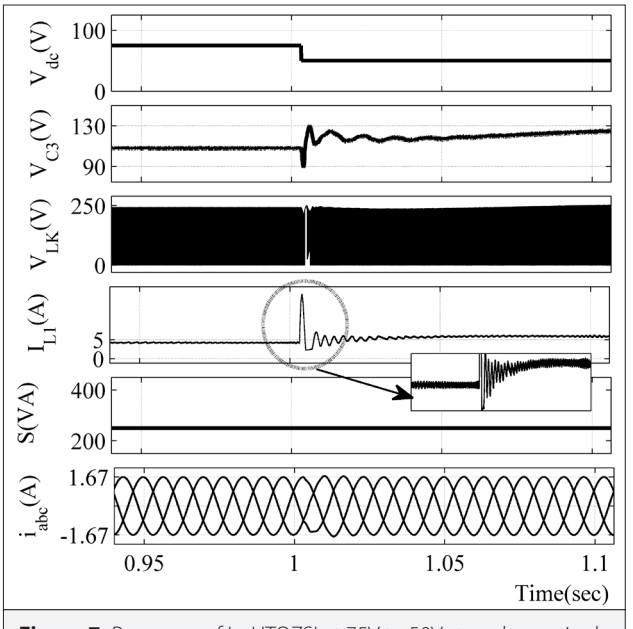

Figure 7. Response of ImHTQZSI at 75V to 50V step change in dc voltage

To better analyze waveforms, they are considered as five case studies to illustrate the transient response. I_{L1} and S are the current through the inductor L_1 and load Volt-Amperes, respectively.

Case i: V_1=25 V, V_2=0 V, V_3=25 V, and V_4=25 V at 250 VA, 0.8 pf load

Out of four dc voltage sources in the converter, V_2 is considered inactive in this case due to general maintenance issues or maintenance issues because of breakdown in the renewable energy extraction system, makes net input voltage is at 75 V (V_{dc}) in the impedance network. Step change in V_{dc} value from 100V to 75V is indicated in the simulation. Change in voltage on dc-side at 0.5 sec results in immediate reduction of capacitor voltage and increases afterward, finally reaching a particular value due to the non-minimum phase phenomena. The dc-link voltage changes in the transient period are observed in Figure 6.

As the V_{dc} is decreased by 25 V, D is increased from 0.143 to 0.173. Hence, the ac per phase output voltage at 70.7 V is maintained uniformly. Correspondingly, capacitor voltage distribution in the network is also varied. Here V_{C3} value is changed to 108.5 V from 116.7 V and V_{LK} is changed to 241.6 V from 233.3 V. As the load on the converter is not changed, there is no change in load current magnitude. Under step change in dc voltage on the input side, based on equation (24), inductor current I_{L1} jumps from 2.5 A to 3.33 A and the transient period continues with the duration from 0.5 sec to 0.6 sec and then the converter stays at the steady-state condition.

Case ii: V_1=25 V, V_2=0 V, V_3=0 V, and V_4=25 V at 250 VA, 0.8 pf load

A step change in voltage from 75 V to 50 V has occurred due to the inactiveness of voltage source V_3 and meets the load Volt-Amperes. The overall change in voltage is from 100 V to 50 V. ImHTQZSI has two dc voltage sources out of four. Two of the dc voltage sources V_2 and V_3 are inactive which makes net input dc voltage V_{dc} as 50 V. Change in voltage on dc-side at the instant 1 sec causes immediate changes in capacitor voltages and the dc-link voltage, and the transient response is observed in Figure 7. As the V_{dc} is decreased by 25 V, D has been increased from 0.173 to 0.2 to maintain the ac per phase output voltage at 70.7 V. Here V_{C3} value has been changed to 125 V from 108.5 V and V_{LK} changed to 250 V from 241.6 V.

In this case, also there are no load changes on the converter as there is no change in i_{abc} magnitude. Under step change in V_{dc}, I_{L1} jumps from 3.33 A to 5 A and the transient period continues with the duration from 1 sec to almost 1.15 sec and then the converter reaches the steady-state condition. Figure 8 shows very low total harmonic distortion (THD) in current waveform on load side during the interval zero sec to 1.5 sec. It is evident from the case i and case ii that the proposed converter can reach the load requirements even when any of the input voltage source is not available which provides flexibility in the maintenance of the input dc voltage source mechanisms.

Case iii: V_1= 25 V, V_2= 0 V, V_3=0 V, and V_4=25 V at 375 VA, 0.8 pf load

As in the previous case, there is no change in dc input voltage but 50% step change of load from 250 VA to 375 VA at 0.8 pf lag occurred at 1.5 sec. It influences I_{L1} *to* increase from 5 A to 7.5 A and also i_{abc} changes from 1.667 A, peak current to 2.5 A, peak value as shown in Figure 9. The load disturbance also causes transient condition on the dc-side. As the *m* and *D* are interdependent on one another, disturbances on either side are transferred and influence performance on both sides. In this case, there is no change in input dc voltage and hence the dc-link voltage and capacitor voltages continue to be as in the previous case.

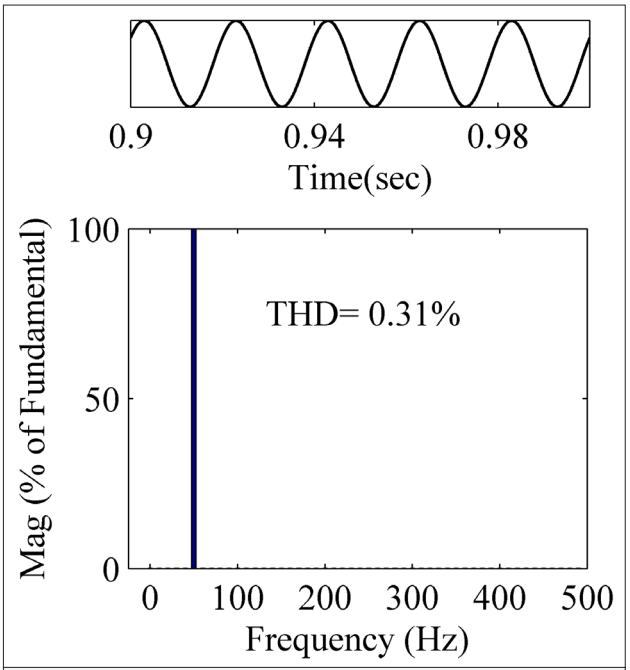

Figure 8. Current THD at 250VA, 0.8pf lag

Case iv: V_1=25 V, V_2=0 V, V_3=25 V, and V_4=25 V at 375 VA, 0.8 pf load

Just as in the previous case, step change in voltage from 50V to 75V is done without any change in load at 2 sec. As the voltage on dc-side increases, I_{L1} will decrease from 7.5 A to 5 A as shown in Figure 10, whereas in case ii voltage decreased to 50 V from 75 V. As there is change in dc voltage, the capacitor voltages and dc-link voltage increases and then decreases and settles at a particular value due to non-minimum phase phenomena. V_{C3} changes from 125 V to 108.5 V and V_{LK} changes to 241.6 V from 250 V, respectively.

It is evident from the case iii and case iv that the proposed converter can overcome the load variations when any one of the input voltage sources is not available.

Case v: V_1=25 V, V_2=25 V, V_3=25 V, and V_4=25 V at 375 VA, 0.8 pf load

In case i the change in dc voltage was decreased whereas in case v it was increased at 2.5 sec, but the loads at both the cases are different. Here all the dc sources have met the load requirements with a change in load from 250 VA to 375 VA as shown in Figure 11. I_{L1} is decreased from 5 A to 3.75 A. Figure 12 shows very less THD in the current waveform on the load side with a peak current value of 2.5 A after 2.5 sec. As dc voltage changes, V_{C3} and V_{LK} are also changed from 108.5 V to 116.7 V and 241.6 V to 233.3 V, respectively.

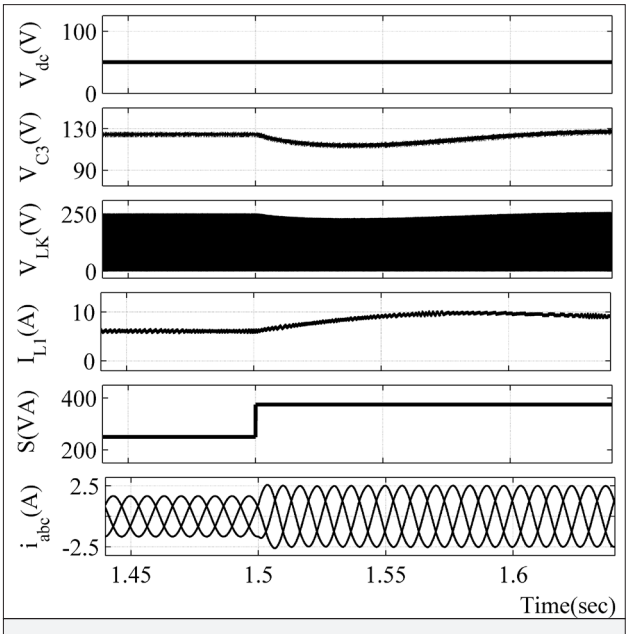

Figure 9. Response of ImHTQZSI for a step change in VA from 250VA to 375VA as well as change in voltage continues

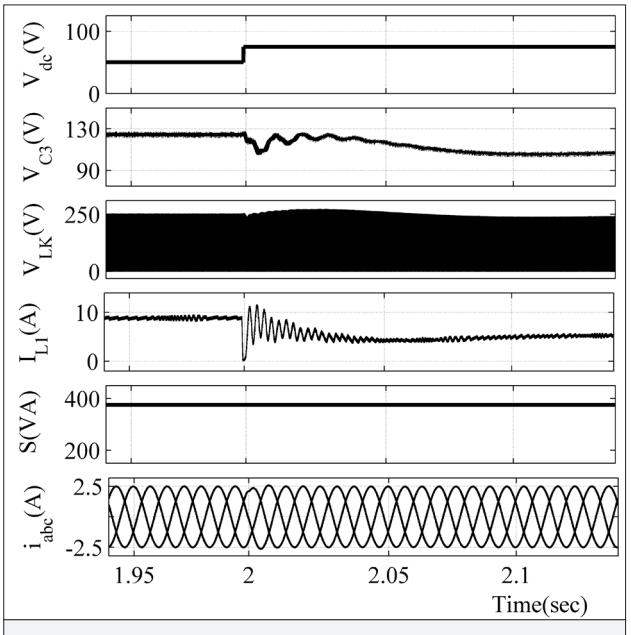

Figure 10. Response of ImHTQZSI for a step change in VA from 250VA to 375VA as well as change in voltage from 50V to 75V

The dc-link voltage V_{LK} has been varying from zero to a peak value as shown in Figure 13. It has a zero value in the shoot-through period and a peak value in the non-shoot-through period. Figure 14 shows the voltage boost factor in comparison with other converters. When *D* is in the range of 0 to 0.25, the proposed converter provides a higher voltage gain. It has been observed that for an incremental step change of input dc voltages or an incremental change in load disturbance can cause overshoots in capacitor and dc-link voltages. Whereas a decrement step change of input dc voltages can cause undershoots in the capacitor and dc-link voltages is observed in Figure 5. It has been observed from all the cases, the converter has been working well to meet load requirements with dual-loop control method even when variations occur in source voltage and load voltage.

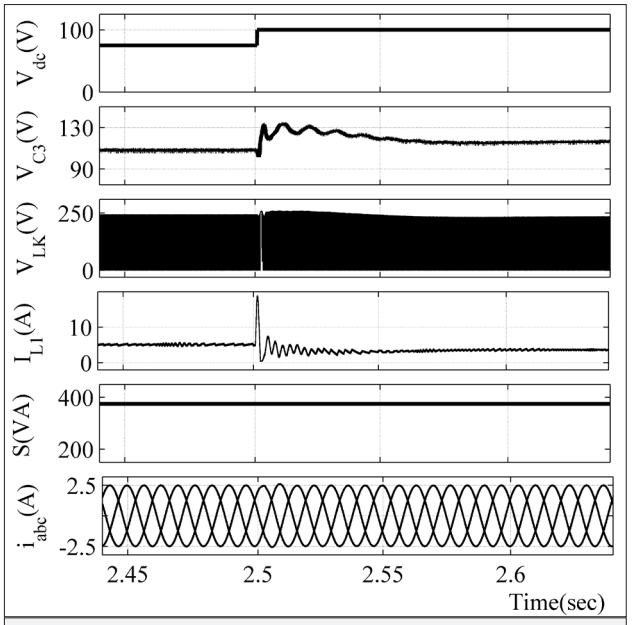

Figure 11. Response of ImHTQZSI for a step change in VA from 250VA to 375VA as well as change in voltage from 75V to 100V

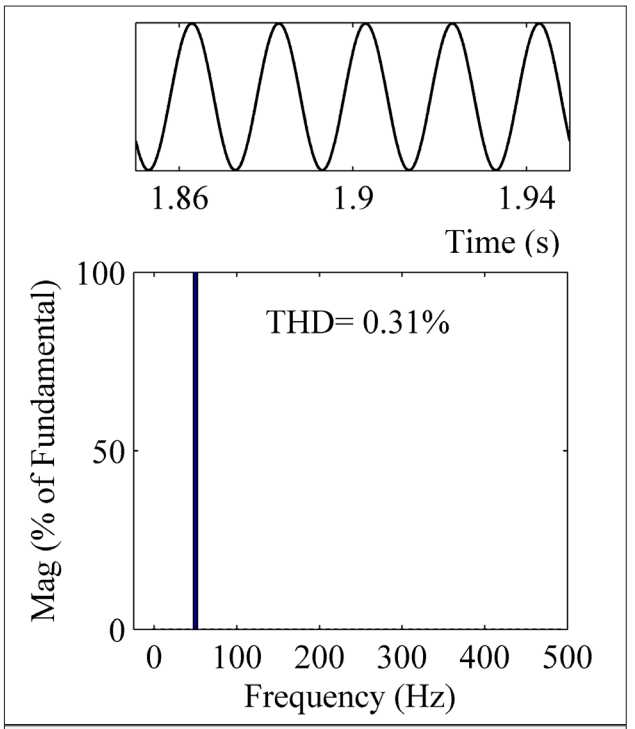

Figure 12. Current THD at 375VA, 0.8pf lag

Conclusion

An implanted hybrid three QZSC has been designed for utilizing its four dc voltage sources efficiently to meet load requirements. This converter is providing higher voltage gain when compared to the non-coupled ISC. The net input dc voltage applied to the converter is the sum of all voltage sources that existed in the converter configuration. The steady-state and dynamic response of the converter has been illustrated with the dual-loop control method. The converter has been providing a constant ac voltage across the load terminals by controlling the dc-link voltage. By controlling capacitor voltage as well as the inductor current ripples with the dual-loop control method on dc-side, we are able to control the dc-link voltage. The controller tracks the reference current on the load side under the sudden change of load on the ac-side as well as the change in net dc voltage. The controller has been providing lower THD in the load current. The converter has been working in the absence

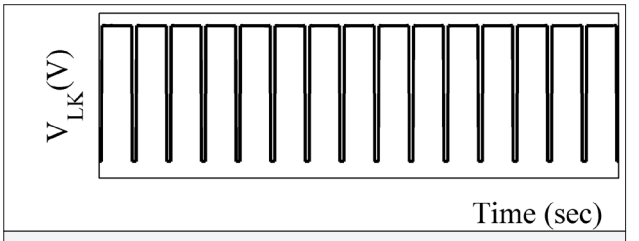

Figure 13. Closed observation of dc-link voltage

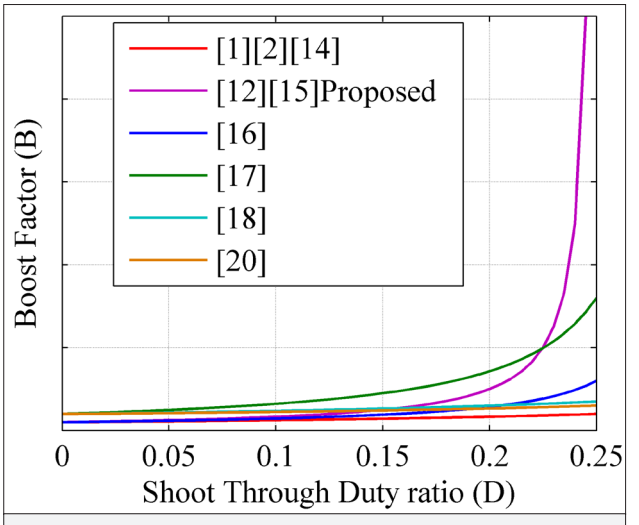

Figure 14. Voltage boost factor comparision among the converters

of any of the voltage sources and so it provides flexibility of operation even when any one of the input source is not available due to maintenance, faults, or any other reason that occur during the energy extraction mechanisms. The four dc voltages are considered to be extracted from various renewable energy sources.

Peer-review: Externally peer-reviewed.

Conflict of Interest: The authors have no conflicts of interest to declare.

Financial Disclosure: The authors declared that this study has received no financial support.

References

1. F. Z. Peng, "Z-source inverter", IEEE Transactions on Industry Applications, vol. 39, No.2, pp. 504-510, March-April, 2003. [CrossRef]
2. J. Anderson, F.Z. Peng, "Four Quasi-Z-Source Inverters", 2008 IEEE Power Electronics Specialists Conference, Rhodes, Greece, August 2008, pp. 2743-2749. [CrossRef]
3. O. Ellabban, H. Abu-Rub, "Z Source Inverter: Topology Improvements Review" IEEE Industrial Electronics magazine, vol.10, No.1, pp. 6-24, March, 2016. [CrossRef]
4. Yam P. Siwakoti, F. Blaabjerg, P. C. Loh, "New Magnetically Coupled Impedance (Z-) Source Networks" IEEE Transactions on Power Electronics, Vol. 31, No. 11, pp. 7419-7435, November, 2016. [CrossRef]
5. Y. P. Siwakoti, P. C. Loh, F. Blaabjerg, G. E. Town, "Effects of Leakage Inductances on Magnetically Coupled Y-Source Network", IEEE Transactions on Power Electronics, Vol. 29, No. 11, pp. 5662-5666, November, 2014. [CrossRef]
6. H. Liu, Z. Zhou, K. Liu, P. C. Loh, W. Wang, D. Xu, F. Blaabjerg, "A Family of High Step-Up Coupled-Inductor Impedance-Source Inverters With Reduced Switching Spikes", IEEE Transactions on Power Electronics, Vol. 33, No. 11, pp. 9116 – 9121, November, 2018. [CrossRef]
7. A. Abdelhakimr, F. Blaabjerg, P. Mattavelli, "Modulation Schemes of the Three-Phase Impedance Source Inverters—Part I: Classification and Review", IEEE Transactions on Industrial Electronics, Vol. 65, No. 8, pp. 6309 – 6320, August, 2018. [CrossRef]
8. O. Ellabban, H. Abu-Rub, "An overview for the Z-Source Converter in motor drive applications", Renewable and Sustainable Energy Reviews Vol.61 pp. 537–555, August, 2016. [CrossRef]
9. J. Zhang, "Unified control of Z-source grid-connected photovoltaic system with reactive power compensation and harmonics restraint: design and application", IET Renewable Power Genereration, Vol. 12, No. 4, pp. 422-429, March, 2018. [CrossRef]
10. Q. Tran, T. Chun, J. Ahn, H. Lee, "Algorithms for Controlling Both the DC Boost and AC Output Voltage of Z-Source Inverter", IEEE Transactions on Industrial Electronics, Vol. 54, No. 5, pp. 2745 – 2750, October, 2007. [CrossRef]
11. H. Liu, P. Liu, Y. Zhang, "Design and digital implementation of voltage and current mode control for the quasi-Z-source converters", IET Power Electronics, Vol. 6, No. 5, pp. 990–998, June, 2013. [CrossRef]
12. H. Shen, B. Zhang, D. Qiu, "Hybrid Z-Source Boost DC–DC Converters", IEEE Transactions Industrial Electronics, Vol. 64, No. 1 pp. 310 – 319, January, 2017. [CrossRef]
13. E. Babaei, E. S. Asl, "A new topology for Z-source half-bridge inverter with low voltage stress on capacitors", Electric Power Systems Research, vol. 140, pp722–734, November, 2016. [CrossRef]
14. P. C. Loh, F. Gao, F. Blaabjerg, "Embedded EZ-Source Inverters", IEEE Transactions on Industry Applications, Vol. 46, No. 1, pp 256 – 267, January-February, 2010. [CrossRef]
15. R. Alla, A. Chowdhury, "An Implanted Hybrid Three Quasi Z source Inverter for Photovoltaic Power Generation Applications", IEEE International Students' Conference on Electrical, Electronics and Computer Science (SCEECS), NIT Bhopal, India February 2018, pp. 1- 6. [CrossRef]
16. V. Jagan, J. Kotturu, S. Das, "Enhanced-Boost Quasi-Z-Source Inverters With Two-Switched Impedance Networks", IEEE Transactions on Industrial Electronics, Vol. 64, No. 9, pp. 6885 – 6897, September, 2017. [CrossRef]
17. X. Zhu, B. Zhang, D. Qiu, "A High Boost Active Switched Quasi-Z-Source Inverter With Low Input Current Ripple", IEEE Transactions on Industrial Informatics, Vol. 15, No. 9, pp. 5341 – 5354, September, 2019. [CrossRef]
18. S. Rostami, V. Abbasi, F. Blaabjerg, "Implementation of a common grounded Z-source DC–DC converter with improved operation factors", IET Power Electronics, Vol. 12, Iss. 9, pp. 2245-2255, August, 2019. [CrossRef]
19. M. H. B. Nozadian, E. Babaei, E. S. Asl, S. H. Hosseini, "Switched Z-source networks: a review", IET Power Electronics, Vol. 12, Iss. 7, pp. 1616-1633, July, 2019. [CrossRef]
20. M. Veerachary, P. Kumar, "Analysis and Design of Sixth Order Quasi-Z-Source DC-DC Boost Converter", IEEE International Conference on Sustainable Energy Technologies and Systems (ICSETS) Bhubaneswar, India February-March, 2019 pp. 347 – 352. [CrossRef]
21. M. Shen, F. Z. Peng, "Operation Modes and Characteristics of the Z-Source Inverter With Small Inductance or Low Power Factor", IEEE Transactions on Industrial Electronics, Vol. 55, No. 1, pp. 89 – 96, January, 2008. [CrossRef]

Ramanjaneyulu Alla received the B.Tech. degree in electrical and electronics engineering from Jawahar Lal Nehru Technological University Hyderabad, India, in 2005, and the M.Tech. degree in Power Electronics from Jawahar Lal Nehru Technological University Kakinada, India, in 2012, Currently he pursuing Ph.D. degree in the Electrical Engineering Department at S.V. National Institute of Technology, Surat in India, from July 2017. His current research interests include power electronics, impedance source converters and its applications.

Anandita Chowdhury received her B.E. and M.E. degree from the University of Calcutta, and the Ph.D. degree from the Indian Institute of Technology, Kharagpur. Presently she is working as Professor in the Department of Electrical Engineering of S. V. National Institute of Technology, Surat, India. She has more than twenty five years of teaching experience. Her area of research interest includes electrical machines, drives and power system stability.